East European Journal of Physics. **4.** 98-108 (2023)
DOI:10.26565/2312-4334-2023-4-10 ISSN 2312-4334

EFFECT OF ARRHENIUS ACTIVATION ENERGY IN MHD MICROPOLAR NANOFLUID FLOW ALONG A POROUS STRETCHING SHEET WITH VISCOUS DISSIPATION AND HEAT SOURCE

Keshab Borah[a]*, Jadav Konch[b†], Shyamanta Chakraborty[c§]
[a] *Department of Mathematics, Gauhati University, Guwahati-781014, Assam, India*
[b] *Department of Mathematics, Dhemaji College, Dhemaji-787057, Assam, India*
[c] *UGC-HRDC, Gauhati University, Guwahati-781014, Assam, India*
**Corresponding Author e-mail: keshabborah388@gmail.com*
[†]*E-mail: jadavkonch@gmail.com;* [§]*E-mail: schakrabortyhrdc@gauhati.ac.in*
Received September 9, 2023; revised October 10, 2023; accepted October 10, 2023

A numerical study of the heat and mass transfer of a micropolar nanofluid flow over a stretching sheet embedded in a porous medium is carried out in this investigation. The main objective of this work is to investigate the influence of Arrhenius activation energy, heat source and viscous dissipation on the fluid velocity, microrotation, temperature, and concentration distribution. The equations governing the flow are transformed into ordinary differential equations using appropriate similarity transformations and solved numerically using bvp4c solver in MATLAB. Graphs are plotted to study the influences of important parameters such as magnetic parameter, porosity parameter, thermophoresis parameter, Brownian motion parameter, activation energy parameter and Lewis number on velocity, microrotation, temperature and concentration distribution. The graphical representation explores that the velocity of the liquid diminishes for increasing values of magnetic parameter, whereas the angular velocity increases with it. This study also reports that an enhancement of temperature and concentration distribution is observed for the higher values of activation energy parameter, whereas the Lewis number shows the opposite behavior. The effects of various pertinent parameters are exposed realistically on skin friction coefficient, Nusselt and Sherwood numbers via tables. A comparison with previous work is conducted, and the results show good agreement.
Keywords: *Arrhenius activation energy; Viscous dissipation; Brownian motion; Thermophoresis; Micropolar nanofluid; Porous medium*
PACS: 44.05.+e; 44.30.+v; 44.20.+b;47.85.-g

INTRODUCTION

The flow and heat transfer characteristics of specific fluids such as polymeric fluids, colloidal fluids, fluids with additives, animal blood, paints, and fluids with suspensions cannot be adequately explained using conventional Newtonian or non-Newtonian fluid flow theories. As a result, Eringen [1] introduced the concept of microfluids, which focuses on a particular category of fluids that demonstrate specific microscopic effects originating from the local structure and micro-motions of the fluid elements. These fluids have the capability to accommodate stress moments and body moments, and their behavior is influenced by spin inertia. Subsequently, Eringen [2] further developed a subclass of these fluids known as micropolar fluids. These fluids exhibit micro-rotational effects and micro-rotational inertia, but they do not possess the ability to undergo stretch.

The study of magnetohydrodynamics (MHD) focuses on the interaction between the fluid velocity field and the electromagnetic field. In recent years, numerous authors have studied about MHD due to its various applications in engineering and industry. For instance, MHD can be utilized in power generators, accelerators, harnessing energy from geothermal sources, and crystal growth. Eldabe *et al.* [3] conducted a numerical study on the heat transfer in magnetohydrodynamic (MHD) flow of a micropolar fluid over a stretching sheet with suction and blowing through a porous medium. They employed the Chebyshev finite difference method (ChFD) to obtain the solution. Using the same method, they [4] also investigated the heat and mass transfer in a hydromagnetic flow of a micropolar fluid past a stretching surface in presence of Ohmic heating and viscous dissipation. Nadeem and Hussain [5] examined the motion of a viscous fluid in a magnetically induced shear field towards a nonlinear porous stretching sheet. Bhattacharyya [6] investigated reactive mass transfer and stable boundary layer flow in an exponentially flowing free stream. Muhaimin and Khamis [7] investigated the heat and mass transport in the context of nonlinear MHD flow of the boundary layer over a shrinking sheet, considering the influence of suction. Mandal and Mukhopadhyay [8] studied the impact of surface heat flux on fluid flow through an exponentially stretching porous sheet. Elbashbeshy [9] examined the heat and mass transfer over a vertical surface with varying temperature in presence of magnetic field.

Hassanien and Gorla [10] conducted a study on the numerical solution for heat transfer in a micropolar fluid over a non-isothermal stretching sheet. Pal and Chatterjee [11] observed the flow of a micropolar fluid in a porous medium toward a heated stretched sheet considering the influence of thermal radiation. Abd El-Aziz [12] examined the influence of viscous dissipation on the mixed convection flow of a micropolar fluid past over an exponentially stretched sheet. Hussain *et al.* [13] investigated the effect of radiation on the thermal boundary layer flow of a micropolar fluid towards a

Cite as: K. Borah, J. Konch, S. Chakraborty, East Eur. J. Phys. 4, 98 (2023), https://doi.org/10.26565/2312-4334-2023-4-10

stretched sheet with permeability. Pal and Mandal [14] investigated the effects of thermal radiation and MHD on the boundary layer flow of a micropolar nanofluid over a stretching sheet with a non-uniform heat sink/source. Kumar [15] performed research on a stretched sheet, employing finite element analysis to examine the heat and mass transfer in a hydromagnetic micropolar flow. Goud *et al.* [16] studied Ohmic heating and the influence of chemical reactions on the MHD flow of a micropolar fluid over a stretching surface.

Micropolar nanofluid is a unique and fascinating class of fluid that combines the characteristics of micropolar fluids and nanofluids. It is a fluid that consists of a base fluid, such as water or oil, in which tiny nanoparticles are dispersed. The presence of nanoparticles in the micropolar nanofluid alters its thermophysical properties, such as thermal conductivity and viscosity. The nanoparticles, due to their small size and large surface area, significantly enhance heat transfer and fluid flow characteristics compared to conventional fluids. This makes micropolar nanofluids highly attractive for various applications involving heat transfer, such as cooling systems, thermal management, and energy conversion devices. Atif *et al.* [17] examined the characteristics of a bio-convective MHD micropolar nanofluid with stratification. They observed that the density distribution decreases when both the density stratification and mixed number parameter are increased. Zemedu and Ibrahim [18] investigated the flow of a micropolar nanofluid with nonlinear convection and multiple slip effects. They concluded that increasing the solutal nonlinear convection parameter results in an increase in velocity.

The flow and heat transport phenomena of nanofluids have attract the researchers due to its various applications in science and engineering. The results of viscous dissipation in a hybrid nanofluid flow with magnetic effects were analyzed by Waini *et al*. [19]. The study found that the Nusselt number decreases for higher values of the Eckert number and radiation parameter in a hybrid nanofluid. In their research, Sharma *et al*. [20] investigated the combined effect of thermophoresis and Brownian motion on magnetohydrodynamic mixed convective flow over an inclined stretching surface, considering the influence of thermal radiation and chemical reaction. Bhatti *et al.* [21] investigated the electro-magneto-hydrodynamic Eyring-Powell fluid flow through microparallel plates, considering heat transfer and non-Darcy effects. Khan *et al*. [22] conducted an investigation on the flow of micropolar base nanofluid over a stretching sheet in the presence of thermal radiation and a magnetic dipole. Recently, Khan *et al*. [23] studied the unsteady micropolar hybrid nanofluid flow past a permeable stretching/shrinking vertical plate. Kausar *et al*. [24] investigated the impact of thermal radiation and viscous dissipation on the boundary layer flow of micropolar nanofluid towards a permeable stretching sheet in porous medium. The influence of thermal radiation and viscous dissipation on a three-dimensional MHD viscous flow were examined by Akbar and Sohail [25].

Activation energy is a critical threshold that must be reached for a chemical reaction to occur. It represents the minimum energy required for the reactants to form products and can be found in the form of kinetic or potential energy. Without this energy, the reaction cannot proceed. Activation energy finds diverse applications in various fields such as geothermal engineering, chemical engineering, oil emulsions, and food processing. In recent years, several researchers have explored their research on the influence of Arrhenius activation energy in boundary layer flow, particularly in the context of non-Newtonian fluid flow, considering different physical aspects. Devi *et al*. [26] studied the impact of various factors, including thermal radiation, buoyancy force, chemical reaction, and activation energy, on the behavior of MHD nanofluid flow past a vertically stretching surface. Li *et al*. [27] observed chemical reaction and activation energy effects on unsteady MHD dissipative Darcy-Forchheimer squeezed flow along a horizontal channel in the context of Casson fluid. In the study conducted by Dessie [28], this study aims to investigate the effects of heat radiation, activation energy and chemical reactions on MHD Maxwell fluid flow in a rotating frame. In a MHD nanofluid flow with double stratification, binary chemical reactions were studied by Anjum *et al*. [29]. Gautam *et al*. [30] explored their investigation on the influence of binary chemical reaction and activation energy in a porous medium for the MHD flow of Williamson nanofluid.

Motivated by the above study, our objective is to investigate the effects of activation energy, viscous dissipation and magnetic field on boundary layer flow of micropolar nanofluid in a porous medium along a stretching sheet in the presence of a heat source. The study of combined influences of activation energy and viscous dissipation in micropolar nanofluid flow induced by a stretching sheet in the presence of heat source and magnetic field is quite a novel problem. The introduction of porous medium along with a magnetic field and heat source makes the physical problem more interesting and attractive in scientific and application viewpoints. Also, numerical solutions are obtained for the governing equations using MATLAB inbuilt function ‘bvp4c’. The graphical and tabular form of the computed results shall be presented and discussed.

MATHEMATICAL FORMULATION

We have considered a steady two-dimensional laminar flow of an incompressible micropolar nanofluid caused by the motion of a stretching sheet. The sheet is immersed in a quiescent, electrically conducting fluid with an electric conductivity represented by σ. A magnetic field B_0 is applied to the stretching sheet. We neglect the influence of the induced magnetic field due to the assumption that the magnetic Reynolds number is too small. Additionally, we assume that there is no impressed electric field and neglect the Hall effect.

Let us define the coordinates such that the *x*-axis aligns with the sheet and the *y*-axis is perpendicular to it. The surface originates from a narrow opening at the origin. The velocity components in the *x* and *y* directions are represented

by *u* and *v*, respectively while *N* represents the microrotation component. It is assumed that the speed of a point on the sheet is inversely proportional to its distance from the opening. Furthermore, we consider the fluid properties to be isotropic and constant. The flow geometry of the problem is depicted in Figure 1.

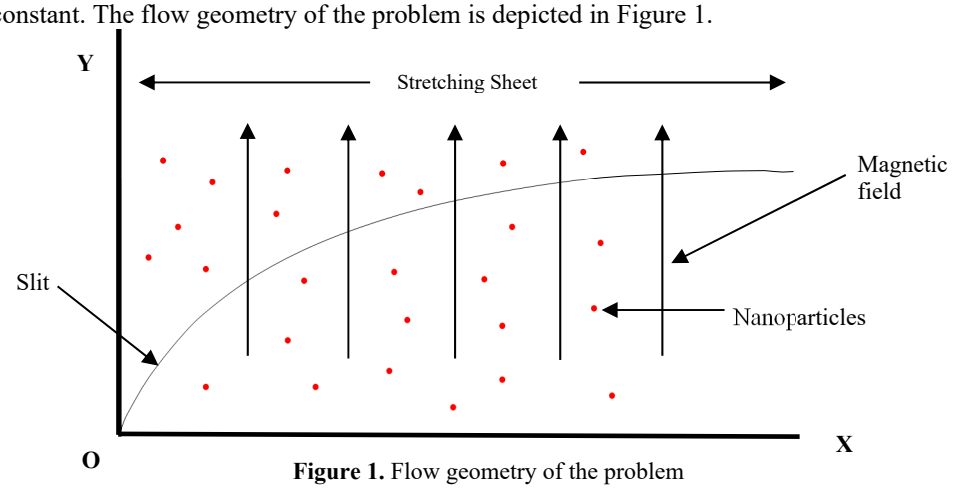

Figure 1. Flow geometry of the problem

Using the typical boundary layer approximation and following Saidulu *et al.* [31] and Rehman *et al.* [32], the governing equations can be expressed as follows:
Continuity Equation:

$$\frac{\partial u}{\partial x}+\frac{\partial v}{\partial y}=0 \tag{1}$$

Momentum Equation:

$$u\frac{\partial u}{\partial x}+v\frac{\partial u}{\partial y}=\left(\frac{\mu+\kappa}{\rho}\right)\frac{\partial^2 u}{\partial y^2}+\frac{\kappa}{\rho}\frac{\partial N}{\partial y}-\frac{\sigma B_0^2 u}{\rho}-\frac{\upsilon}{k_p'}u \tag{2}$$

Angular momentum Equation:

$$u\frac{\partial N}{\partial x}+v\frac{\partial N}{\partial y}=\frac{\gamma}{\rho j}\frac{\partial^2 N}{\partial y^2}-\frac{\kappa}{\rho j}\left(2N+\frac{\partial u}{\partial y}\right) \tag{3}$$

Energy Equation:

$$u\frac{\partial T}{\partial x}+v\frac{\partial T}{\partial y}=\frac{k_f}{\rho C_p}\frac{\partial^2 T}{\partial y^2}+\left(\frac{\mu+\kappa}{\rho C_P}\right)\left(\frac{\partial u}{\partial y}\right)^2+\frac{\sigma B_0^2}{\rho C_p}u^2+\frac{Q_0}{\rho C_p}(T-T_\infty)+\tau\left(D_B\frac{\partial C}{\partial y}\frac{\partial T}{\partial y}+\frac{D_T}{T_\infty}\left(\frac{\partial T}{\partial y}\right)^2\right) \tag{4}$$

Concentration Equation:

$$u\frac{\partial C}{\partial x}+v\frac{\partial C}{\partial y}=D_B\frac{\partial^2 C}{\partial y^2}+\frac{D_T}{T_\infty}\frac{\partial^2 T}{\partial y^2}-k_r^2\left(\frac{T}{T_\infty}\right)^n e^{-\frac{E_a}{\xi T}}(C-C_\infty) \tag{5}$$

The suitable physical boundary conditions are:

$$\left.\begin{aligned} &u=u_w=bx,\ v=0,\ N=-s\frac{\partial u}{\partial y},\ T=T_w,\ C=C_w \quad \text{at} \quad y=0\\ &u=0,\quad N=0,\quad T=T_\infty,\quad C=C_\infty \quad \text{as} \quad y\to\infty \end{aligned}\right\} \tag{6}$$

In the above governing equations (4) and (5), the term $\frac{\sigma B_0^2}{\rho C_p}u^2$ represent Ohmic heating effect and the term $k_r^2\left(\frac{T}{T_\infty}\right)^n e^{-\frac{E_a}{\xi T}}(C-C_\infty)$ depicts the modified Arrhenius function, in which the reaction rate is provided by k_r^2, the activation energy by E_a, the Boltzmann constant by $\xi=8.61\times10^{-5}\,eV/K$, and the fitted rate constant by '*n*', which ranges between –1 and 1. Also the spin gradient viscosity, given by Rees and Pop [33], is $\gamma=(\mu+\kappa/2)j$, where j is the microinertia density given by $j=\upsilon/b$ that represent the reference length.

To convert the governing equations into a system of ordinary differential equations, we will employ similarity transformations and introduce dimensionless variables as follows:

$$\eta=\sqrt{\frac{b}{\upsilon}}y,\quad f(\eta)=\frac{\psi}{x\sqrt{b\upsilon}},\quad G(\eta)=\sqrt{\frac{\upsilon}{b}}\frac{N}{bx},\ \theta(\eta)=\frac{T-T_\infty}{T_w-T_\infty},\ \phi(\eta)=\frac{C-C_\infty}{C_w-C_\infty} \tag{7}$$

We have $u=\frac{\partial\psi}{\partial y}$, $v=-\frac{\partial\psi}{\partial x}$, where ψ is the stream function, which gives $u=xbf'(\eta)$ and $v=-\sqrt{b\upsilon}\,f(\eta)$.

We observe that equation (1) is satisfied automatically and equations (2) – (5) are simplified to the following

$$(1+K)f'''-(f')^2+ff''+KG'-\left(M+\frac{1}{K_p}\right)f'=0 \tag{8}$$

$$\left(1+\frac{K}{2}\right)G''+fG'-f'G-K(2G+f'')=0 \tag{9}$$

$$\theta''+\Pr f\theta'+(1+K)\Pr Ec(f'')^2+\Pr Ec\,M(f')^2+\Pr Q\theta+\Pr N_b\theta'\phi'+\Pr N_t(\theta')^2=0 \tag{10}$$

$$\phi''+Le\,f\phi'+\frac{N_t}{N_b}\theta''-Le\wedge(1+\delta\theta)^n\,Exp\left(-\frac{E}{1+\delta\theta}\right)\phi=0 \tag{11}$$

Corresponding boundary conditions are reduced to the following:

$$\left.\begin{array}{l} f(\eta)=0\ ,\ f'(\eta)=1\ ,\ G(\eta)=-s\,f''(\eta)\ ,\ \theta(\eta)=1\ ,\ \phi(\eta)=1\ \text{at}\ \eta=0 \\ f'(\eta)=0\ ,\qquad G(\eta)=0,\qquad \theta(\eta)=0\ ,\qquad \phi(\eta)=0\quad \text{as}\ \eta\to\infty \end{array}\right\} \tag{12}$$

The non-dimensional parameters are defined as follows:

$$K=\frac{\kappa}{\mu}\ ,\ M=\frac{\sigma B_0^2}{\rho b},\ K_p=\frac{k_p'b}{\upsilon},\ \Pr=\frac{\mu C_p}{k_f},\ Ec=\frac{u_w^2}{C_P(T_w-T_\infty)},\ N_b=\frac{\tau D_B(C_w-C_\infty)}{\upsilon},$$

$$N_t=\frac{\tau D_T(T_w-T_\infty)}{\upsilon T_\infty},\qquad Le=\frac{\upsilon}{D_B},\qquad \wedge=\frac{k_r^2}{b},\qquad \delta=\frac{T_w-T_\infty}{T_\infty},\qquad E=\frac{E_a}{\xi T_\infty}.$$

K is the material parameter, M is the magnetic parameter, K_p is the porosity parameter, $\Pr$ is the Prandtl number, Ec is the Eckert number, N_t is the thermophoresis parameter, N_b is the Brownian motion parameter, Le is the Lewis number, $\wedge$ is the reaction rate parameter, E is the activation energy parameter, δ is the temperature difference parameter.

PHYSICAL QUANTITIES

In this problem, the important engineering physical quantities are C_f (=skin friction coefficient), *Nu* (=local Nusselt number) and *Sh* (=local Sherwood number) respectively are defined below with $Re=\frac{bx^2}{\upsilon}$ as local Reynolds number.

The shear stress at the surface is determined by the equation $\tau_w=\left[(\mu+\kappa)\frac{\partial u}{\partial y}+\kappa N\right]_{y=0}$.

The skin friction coefficient (C_f) can be defined as $C_f=\frac{\tau_w}{\rho u_w^2}$, where $u_w=bx$ is characteristic velocity.

This gives

$$C_f=\frac{\left[1+(1-s)K\right]f''(0)}{\sqrt{Re}}$$

The couple stress (M_w) at the surface is defined by the following equation:

$$M_w=\left(\gamma\frac{\partial N}{\partial y}\right)_{y=0}=\mu u_w\left(1+\frac{K}{2}\right)G'(0).$$

The local surface heat flux $q_w(x)$ can be expressed using Fourier's law as:

$$q_w(x)=-k_f\left(\frac{\partial T}{\partial y}\right)_{y=0}=-k_f(T_w-T_\infty)\sqrt{\frac{b}{\upsilon}}\,\theta'(0).$$

The local surface heat flux transfer coefficient $h(x)$ can be given by:

$$h(x)=\frac{q_w(x)}{(T_w-T_\infty)}=-k_f\sqrt{\frac{b}{\upsilon}}\,\theta'(0).$$

The local Nusselt number can be expressed as:

$$Nu = \frac{x\,h(x)}{k_f} = -x\sqrt{\frac{b}{\upsilon}}\,\theta'(0) \quad \text{which gives} \quad \frac{Nu}{\sqrt{Re}} = -\theta'(0)$$

The local mass flux J_w is given by $J_w = -D\left(\frac{\partial C}{\partial y}\right)_{y=0}$.

The Sherwood number can be expressed as follows:

$$Sh = \frac{x\,J_w}{D\left(C_w - C_\infty\right)} = -x\sqrt{\frac{b}{\upsilon}}\,\phi'(0) \quad \text{which gives} \quad \frac{Sh}{\sqrt{Re}} = -\phi'(0)$$

METHOD OF SOLUTION

The nonlinear ordinary differential equations, represented by equations (8) to (11) and subject to the boundary conditions (12) are numerically solved using MATLAB inbuilt function 'bvp4c'. It utilizes a finite difference approach with fourth-order accuracy.

To employ the solver effectively, the equations need to be transformed into a system of equivalent first-order ordinary differential equations. This transformation is achieved through the following substitutions:

$$y(1) = f$$
$$y(1)' = f' = y(2)$$
$$y(2)' = f'' = y(3)$$
$$y(3)' = f''' = \frac{[\,y(2)^2 - y(1)\,y(2) - K\,y(5) + (M + 1/Kp)\,y(2)]}{(1+K)}$$
$$y(4) = G$$
$$y(4)' = G' = y(5)$$
$$y(5)' = G'' = \frac{[\,y(4)y(2) - y(1)y(5) + K(2y(4) + y(3))]}{\left(1 + \frac{K}{2}\right)}$$
$$y(6) = \theta$$
$$y(6)' = \theta' = y(7)$$
$$y(7)' = \theta'' = -\Pr\,y(1)y(7) - (1+K)\Pr\,Ec\,y(3)^2 - \Pr\,Ec\,M\,y(2)^2 - \Pr\,Q\,y(6) - \Pr\,Nb\,y(7)\,y(9) - \Pr\,Nt\,y(7)^2$$
$$y(8) = \phi$$
$$y(8)' = \phi' = y(9)$$
$$y(9)' = \phi'' = -Le\,y(1)\,y(9) - (Nt/Nb)\left(y(7)'\right) + y(8)\,e^{\left(-\frac{E}{1+\delta y(6)}\right)}Le \wedge (1+\delta y(6))^n$$

The corresponding boundary conditions are reduced to:

$y0(1) - 0;\ y0(2) - 1;\ y0(4) + s\,y0(3);\ \ y0(6) - 1;\ y0(8) - 1;\ \ y1(2) - 0;\ \ y1(4) - 0;\ \ y1(6) - 0;\ y1(8) - 0$.

RESULTS AND DISCUSSION

The system of non-linear coupled governing boundary layer equations (8)–(11) along with the corresponding boundary conditions (12) is numerically solved using the 'bvp4c' solver in MATLAB. The 'bvp4c' solver is a commonly used tool for solving boundary value problems. This solution satisfies the specified boundary conditions and provides an approximation for the desired variables in the problem. The findings are compared with the findings obtained by Saidulu *et al*. [31], Grubka and Bobba [34] and Seddeek and Salem [35] to verify the accuracy of the present numerical scheme as shown in Table 1 and Table 2.

Figures (2) to (17) depict the variation in velocity distribution, angular velocity distribution, temperature distribution, and species concentration distribution for various flow parameter.

Figures (2) to (5) illustrate the effect of magnetic parameter M on the velocity, angular velocity, temperature and species concentration profile respectively. Figure 2 shows that as the magnetic parameter M increases, the velocity decreases. This is due to the presence of a transverse magnetic field, which creates a resistive force called Lorentz force that acts in the opposite direction to the fluid motion. This observation indicates that a stronger magnetic field has the effect of slowing down the movement of the fluid. Consequently, the thickness of the velocity boundary layer decreases with an increasing M. Figure 3 indicates that angular velocity increases with the increasing values of M. Figure 4 depicts the temperature distribution with respect to the magnetic field parameter. It is observed that the temperature increases as

M increases. This observed phenomenon can be attributed to the influence of the Lorentz force, which resist velocity of the fluid, as a result a rise in temperature. Figure 5 depicts the influence of magnetic parameters on the concentration profile. It is found that the fluid concentration is rising as the magnetic parameter rises.

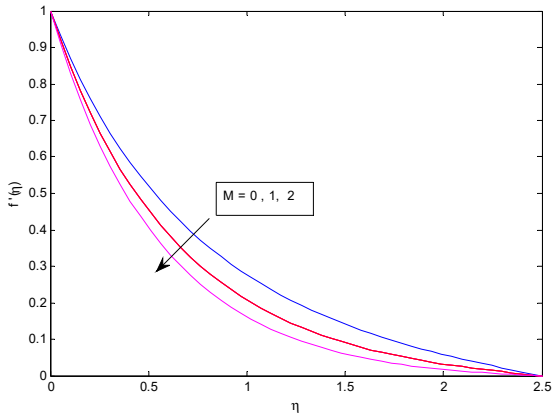

Figure 2. Velocity profile for different *M*.

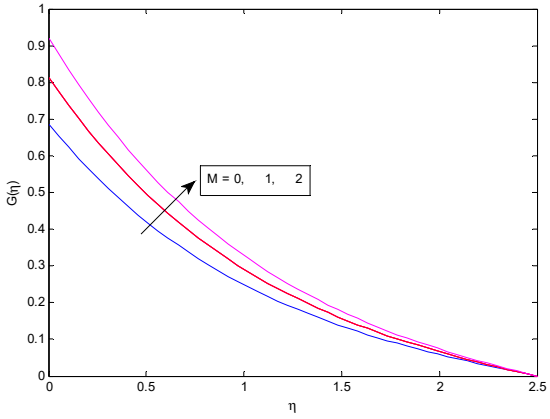

Figure 3. Angular velocity profile for different *M*

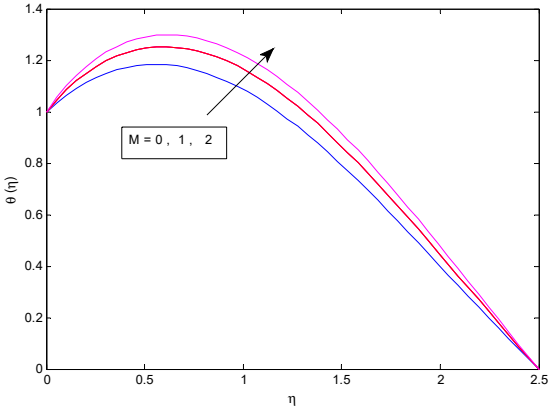

Figure 4. Temperature profile for different *M*

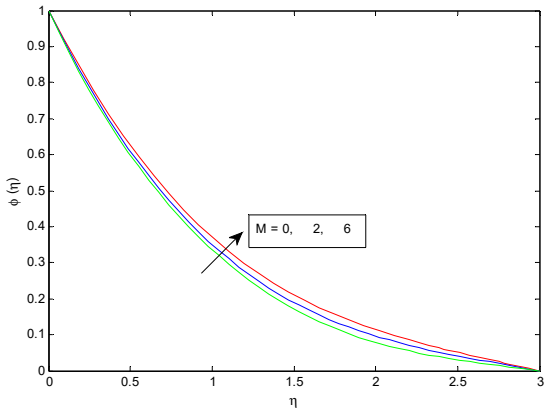

Figure 5. Concentration profile for different *M*

Figures 6–9 illustrate the impact of the porosity parameter *Kp* on various fluid properties, including fluid velocity, angular velocity, fluid temperature, and fluid concentration respectively. It can be observed from figure 6 that as the porosity parameter increases, the fluid is provided with more space to flow, resulting in an increase in fluid velocity. On the other hand, Figures 7–9 clearly demonstrate that an increase in the porosity parameter leads to a decrease in the flow profiles of the micro-rotation, temperature and concentration. Physically, the porosity parameter influences the generation of internal heat within the flow, which contributes to the observed trends in temperature profiles. Additionally, the rotational effects in the flow can contribute to the depreciation observed in the temperature and concentration fields.

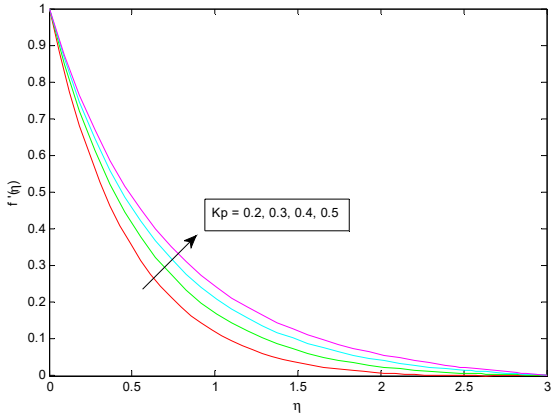

Figure 6. Velocity profile for different *Kp*

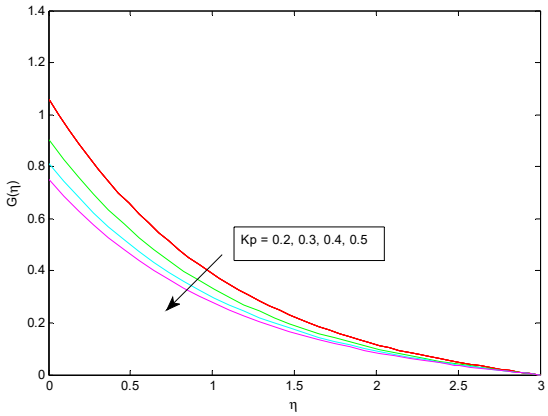

Figure 7. Angular velocity profile for different *Kp*

Figures 10 and 11 depicts the impact of activation energy (*E*) on fluid temperature and fluid concentration, respectively. From Figure 10, it can be observed that an increase in activation energy (*E*) leads to an increase in the

temperature profile. As the temperature increases, the speed of molecular motion increases, resulting in more frequent collisions between molecules. Additionally, the molecules possess higher kinetic energy at higher temperatures. Consequently, the proportion of collisions capable of surpassing the activation energy for the reaction also increases with temperature. Also Figure 11 exhibits that activation energy (E) enhances the fluid concentration. The increasing values of activation energy (E) retard the Arrhenius energy function, which result, increasing the rate of the generative chemical reaction that enhances the concentration.

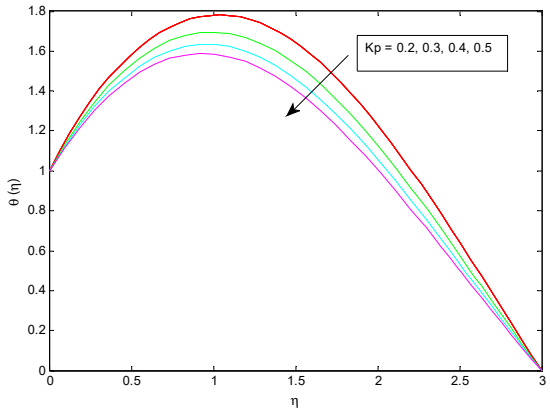

Figure 8. Temperature profile for different Kp

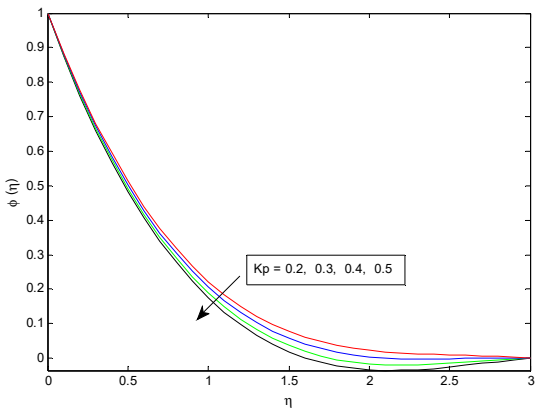

Figure 9. Concentration profile for different Kp

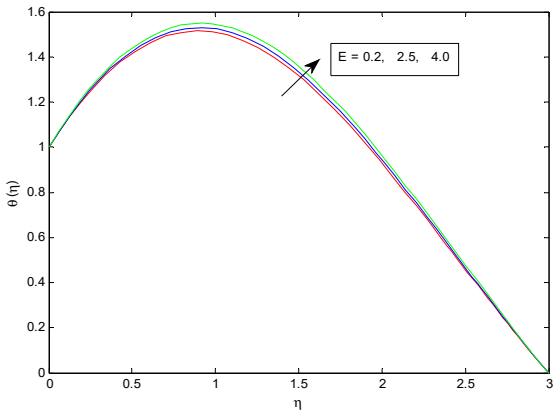

Figure 10. Temperature profile for different E

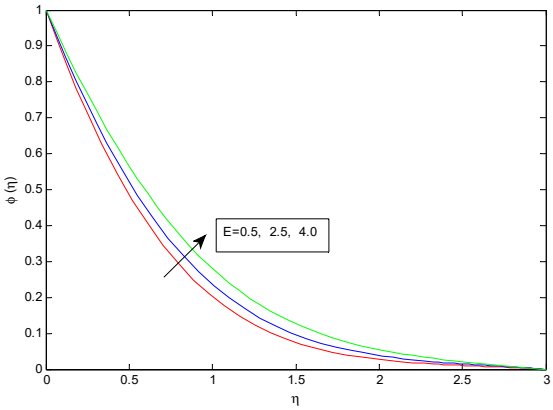

Figure 11. Concentration profile for different E

The Lewis number, which is a dimensionless quantity measuring the rate of temperature spread compared to mass diffusivity, plays a role in the temperature and concentration profiles. In Figure 12 and 13, it can be observed that as the Lewis number (Le) increases, the temperature and concentration profiles decrease. Higher values of Le indicate stronger molecular motions, which ultimately lead to an enhancement in fluid temperature.

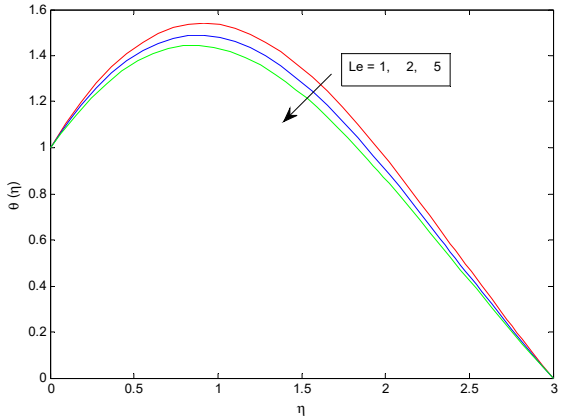

Figure 12. Temperature profile for different Le

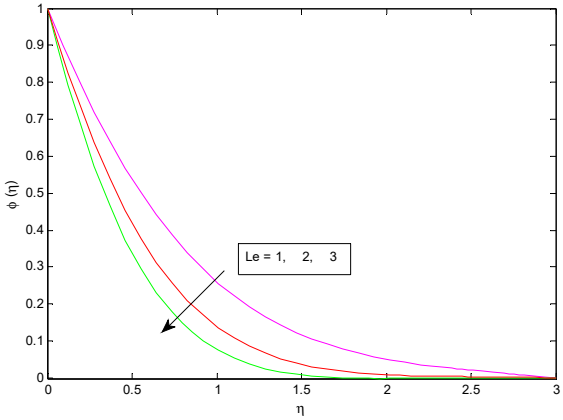

Figure 13. Concentration profile for different Le

Thermophoresis refers to the particle diffusion phenomenon resulting from a temperature gradient. The thermophoretic force is the force that causes nanoparticles to deposit into the surrounding fluid due to the temperature

gradient. For higher values of the thermophoresis parameter N_t, it is observed from the graphs 14 and 15 that both the concentration and temperature profiles are increases. Physically, when $\theta(\eta)$ increases, it leads to a higher thermal gradient, which in turn increases the intermediate force. This relationship is evident in the increasing values of the thermophoresis parameter.

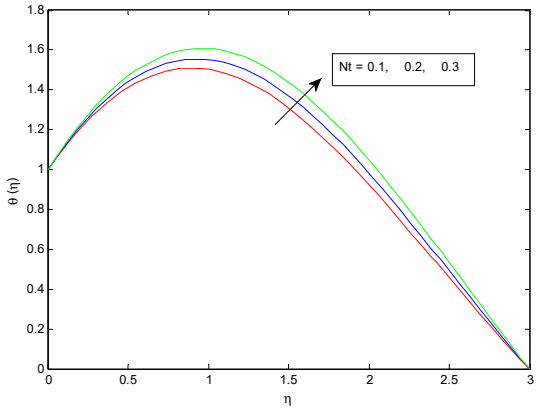

Figure 14. Temperature profile for different N_t

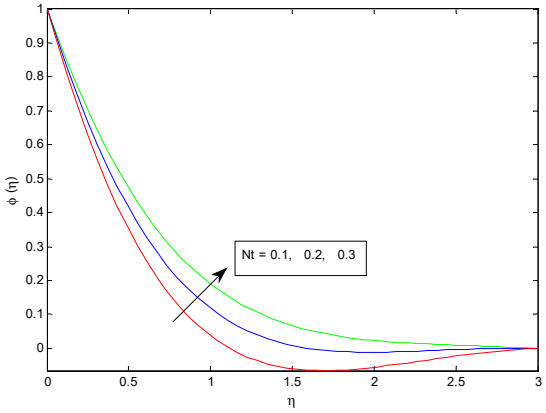

Figure 15. Concentration profile for different N_t

The Brownian motion is created by the random collisions between small particles. The parameter N_b quantifies the level of random motion of suspended nanoparticles within the nanofluid. It is observed that increasing convection leads to enhanced heat transfer, as depicted in Fig. 16. Moreover, the concentration profile decreases as the distance from the surface increases, as shown in Fig. 17. Physically, an increase in temperature results in higher particle energy, leading to greater random movement and faster collisions, thereby increasing the Brownian motion. Conversely, increasing the concentration reduces the available space for particle movement, thereby decreasing the probability of collision.

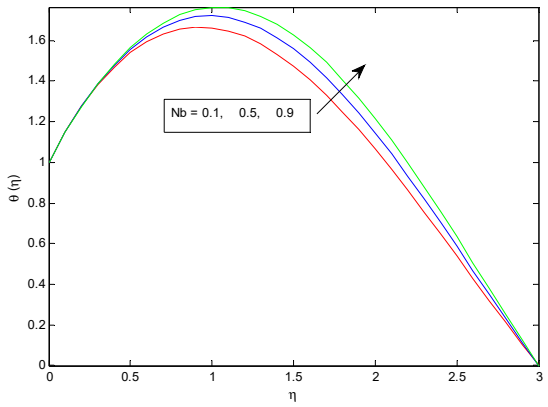

Figure 16. Temperature profile for different N_b

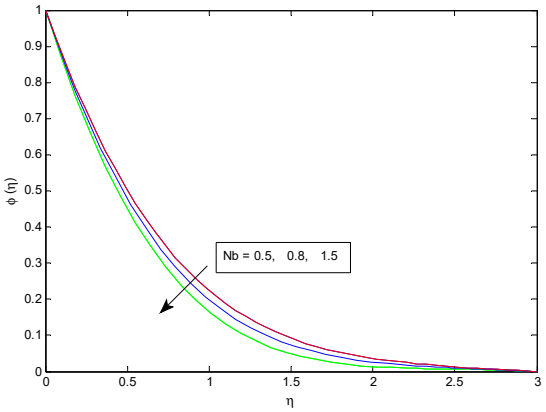

Figure 17. Concentration profile for different N_b

Table 1 illustrates the changes in skin friction coefficient, Nusselt number and Sherwood number due to the parameter M, K and s. It is found that the skin friction coefficient increases with higher values of M, K and s, while opposite effect is observed for the Nusselt number. Also, Sherwood number decreases with an increase in M, but increases with K and s. Table 2 provides a comparison of $-\theta'(0)$ for various values of Pr in the absence of other influencing factors. It is observed that Nusselt number increases with Pr.

Table 1. Comparison of skin friction coefficient, Nusselt number, and Sherwood number for various parameters.

M	K	s	$-(1+K)f''(0)$		$-\theta'(0)$		$-\phi'(0)$	
			Saidulu *et al.* [31]	Present Study	Saidulu *et al.* [31]	Present Study	Saidulu *et al.* [31]	Present Study
0.5	0.5	0.5	1.632309	1.632313	0.301208	0.301234	0.418950	0.418943
1			1.874420	1.874426	0.223923	0.223941	0.400290	0.400297
2			2.276598	2.276568	0.104321	0.104335	0.375010	0.375025
0.5	1		1.983995	1.983981	0.293786	0.293759	0.430439	0.430424
	2		2.576759	2.576779	0.280081	0.280065	0.448508	0.448521
	0.5	0.7	1.983995	1.983967	0.293786	0.293771	0.430439	0.430446
		1	2.295365	2.295332	0.286817	0.286829	0.440171	0.440147

Table 2. Comparison of $-\theta'(0)$ for different values of *Pr*

Pr	Grubka and Bobba [34]	Seddeek and Salem [35]	Saidulu and Reddy [31]	Present Study
0.72	0.4631	0.46134	0.4632	0.4637
1	0.582	0.58197	0.5819	0.58192
3	1.1652	1.16524	1.1652	1.16528

CONCLUSIONS

In this study, the two-dimensional MHD micropolar nanofluid flow over a stretching sheet embedded in a porous medium in the presence of Arrhenius activation energy, heat source is studied. The governing partial differential equations were transformed into a system of ordinary differential equations using a set of similarity transformations. These equations were then solved numerically using the 'bvp4c' solver available in MATLAB. The results of the study led to the following conclusions**:**

- For increasing values of the magnetic field parameter (*M*), the velocity profile decreases. However, the microrotation, temperature, and concentration profiles are strengthened.
- The fluid temperature and concentration profile are enhanced with the increasing values of thermophoresis parameter (N_t).
- The temperature profile increases with the strengthening of the Brownian motion parameter (N_b), while the concentration profile decreases with N_b.
- An increase in activation energy (*E*) leads to an increase in the concentration and temperature profiles.
- Increasing values of the Lewis number (*Le*) result in decreasing temperature and concentration profiles.
- The rate of heat transfer decreases with an enhancement of the magnetic parameter and material parameter.
- The rate of mass transfer, in terms of Sherwood number, decreases with an increase in *M*, but an opposite effect is observed with *K*.

ORCID

Keshab Borah, https://orcid.org/0009-0005-5486-5784; **Jadav Konch,** https://orcid.org/0000-0002-6953-3679
Shyamanta Chakraborty, https://orcid.org/0000-0001-5839-4856

REFERENCES

[1] A.C. Eringen, "Simple Microfluids," International Journal of Engineering Science, **2**(2), 205-217 (1964**)**. https://doi.org/10.1016/0020-7225(64)90005-9
[2] A.C. Eringem, "Theory of Micropolar Fluids," Journal of Mathematics and Mechanics, **16**(1), 1–18 (1966**)**. http://dx.doi.org/10.1512/iumj.1967.16.16001
[3] N.T. Eldabe, E.F. Elshehawey, M.E. Elbarbary, and N.S. Elgazery, "Chebyshev Finite Difference Method for MHD Flow of a Micropolar Fluid past a Stretching Sheet with Heat Transfer," Journal of Applied Mathematics and Computation, **160**, 437-450 (2005**)**. https://doi.org/10.1016/j.amc.2003.11.013
[4] N.T. Eldabe, and E.M.O. Mahmoud, "Chebyshev Finite Difference Method for Heat and Mass Transfer in a Hydromagnetic Flow of a Micropolar Fluid Past a Stretching Surface with Ohmic Heating and Viscous Dissipation," Applied Mathematics and Computation, **177**, 561-571 (2006). https://doi.org/10.1016/j.amc.2005.07.071
[5] S. Nadeem, and A. Hussain, "MHD flow of a viscous fluid on a nonlinear porous shrinking sheet with homotopy analysis method," Appl. Math. Mech.-Engl. **30**, 1569–1578 (2009). https://doi.org/10.1007/s10483-009-1208-6
[6] K. Bhattacharyya, "Steady boundary layer flow and reactive mass transfer past an exponentially stretching surface in an exponentially moving free stream," Journal of the Egyptian Mathematical Society, **20**(3), 223-228 (2012). https://doi.org/10.1016/j.joems.2012.08.018.
[7] R. Muhaimin, Kandasamy, and A.B. Khamis, "Effects of heat and mass transfer on nonlinear MHD boundary layer flow over a shrinking sheet in the presence of suction," Applied Mathematics and Mechanics, **29**, 1309–1317 (2008). https://doi.org/10.1007/s10483-008-1006-z
[8] I.C. Mandal, and S. Mukhopadhyay, "Heat transfer analysis for fluid flow over an exponentially stretching porous sheet with surface heat flux in porous medium," Ain Shams Engineering Journal, **4**(1), 103-110 (2013). https://doi.org/10.1016/j.asej.2012.06.004.
[9] E.M. Elbashbeshy, "Heat and mass transfer along a vertical plate with variable surface tension and concentration in the presence of the magnetic field," International Journal of Engineering Science, **35**, 515-522 (1997). https://doi.org/10.1016/S0020-7225(96)00089-4
[10] I.A. Hassanien, and R.S.R. Gorla, "Heat transfer to a micropolar fluid from a non-isothermal stretching sheet with suction and blowing," Acta Mechanica, **84**, 191–199 (1990**)**. https://doi.org/10.1007/BF01176097
[11] D. Pal, and S. Chatterjee, "MHD mixed convection stagnation-point flow of a micropolar fluid in a porous medium towards a heated stretching sheet with thermal radiation," Mathematical Modelling and Analysis, **17**(4), 498-518 (2012). https://doi.org/10.3846/13926292.2012.706653

[12] M.A. El-Aziz, "Viscous dissipation effect on mixed convection flow of a micropolar fluid over an exponentially stretching sheet," Canadian Journal of Physics, **87**(4), 359-368 (2009). https://doi.org/10.1139/P09-047
[13] M. Hussain, M. Ashraf, S. Nadeem, and M. Khan, "Radiation effects on the thermal boundary layer flow of a micropolar fluid towards a permeable stretching sheet," Journal of the Franklin Institute, **350**(1), 194-210 (2013). https://doi.org/10.1016/j.jfranklin.2012.07.005
[14] D. Pal, and G. Mandal, "Thermal radiation and MHD effects on boundary layer flow of micropolar nanofluid past a stretching sheet with non-uniform heat source/sink," International Journal of Mechanical Sciences, **126**, 308-318 (2017). https://doi.org/10.1016/j.ijmecsci.2016.12.023
[15] L. Kumar, "Finite Element Analysis of Combined Heat and Mass Transfer in Hydromagnetic Micropolar Flow along a Stretching Sheet," Computational Materials Science, **46**, 841-848 (2009). http://dx.doi.org/10.1016/j.commatsci.2009.04.021
[16] B.S. Goud, and M.M. Nandeppanavar, "Ohmic heating and chemical reaction effect on MHD flow of micropolar fluid past a stretching surface," Partial Differential Equations in Applied Mathematics, **4**, 100104 (2021). https://doi.org/10.1016/j.padiff.2021.100104
[17] S.M. Atif, S. Hussain, and M. Sagheer, "Magnetohydrodynamic stratified bioconvective flow of micropolar nanofluid due to gyrotactic microorganisms," AIP Advances, **9**(2), 025208 (2019). https://doi.org/10.1063/1.5085742
[18] C. Zemedu, and W. Ibrahim, "Nonlinear Convection Flow of Micropolar Nanofluid due to a Rotating Disk with Multiple Slip Flow," Mathematical Problems in Engineering, **2020**, 4735650 (2020). https://doi.org/10.1155/2020/4735650
[19] I. Waini, A. Ishak, and I. Pop, "Radiative and magnetohydrodynamic micropolar hybrid nanofluid flow over a shrinking sheet with Joule heating and viscous dissipation effects," Neural Comput & Applic, **34**, 3783–3794 (2022). https://doi.org/10.1007/s00521-021-06640-0
[20] B.K. Sharma, U. Khanduri, N.K. Mishra, and K.S. Mekheimer, "Combined effect of thermophoresis and Brownian motion on MHD mixed convective flow over an inclined stretching surface with radiation and chemical reaction," International Journal of Modern Physics B, **37**, 2350095 (2022). http://dx.doi.org/10.1142/S0217979223500959
[21] M.M. Bhatti, M.H. Doranehgard, and R. Ellahi, "Electro-magneto-hydrodynamic Eyring-Powell fluid flow through micro-parallel plates with heat transfer and non-Darcian effects," Mathematical Methods in the Applied Sciences, **46**(1), 11642-11656 (2022). http://dx.doi.org/10.1002/mma.8429
[22] S.A. Khan, B. Ali, C. Eze, K.T. Lau, L. Ali, J. Chen, and J. Zhao, "Magnetic dipole and thermal radiation impacts on stagnation point flow of micropolar based nanofluids over a vertically stretching sheet: finite element approach," Processes, **9**(7), 1089 (2021). https://doi.org/10.3390/pr9071089
[23] U. Khan, A. Zaib, I. Pop, S.A. Bakar, and A. Ishak, "Unsteady micropolar hybrid nanofluid flow past a permeable stretching/shrinking vertical plate," Alexandria Engineering Journal, **61**(12), 11337-11349 (2022). https://doi.org/10.1016/j.aej.2022.05.011
[24] M.S. Kausar, A. Hussanan, M. Waqas, and M. Mamat, "Boundary layer flow of micropolar nanofluid towards a permeable stretching sheet in the presence of porous medium with thermal radiation and viscous dissipation," Chinese Journal of Physics, **78**(6), 435–452 (2022). http://dx.doi.org/10.1016/j.cjph.2022.06.027
[25] S. Akbar, and M. Sohail, "Three Dimensional MHD Viscous Flow under the Influence of Thermal Radiation and Viscous Dissipation," International Journal of Emerging Multidisciplinaries: Mathematics, **1**(3), 106–117 (2022). https://doi.org/10.54938/ijemdm.2022.01.3.122
[26] G.L. Devi, H. Niranjan, and S. Sivasankaran, "Effects of chemical reactions, radiation, and activation energy on MHD buoyancy induced nanofluid flow past a vertical surface," Scientia Iranica, **29**(1), 90-100 (2022). https://doi.org/10.24200/sci.2021.56835.4934
[27] S. Li, K. Raghunath, A. Alfaleh, F. Ali, A. Zaib, M.I. Khan, S. M. ElDin, and V. Puneeth, "Effects of activation energy and chemical reaction on unsteady MHD dissipative Darcy–Forchheimer squeezed flow of Casson fluid over horizontal channel," Scientific Reports, **13**, 2666, (2023). https://doi.org/10.1038/s41598-023-29702-w
[28] H. Dessie, "Effects of Chemical Reaction, Activation Energy and Thermal Energy on Magnetohydrodynamics Maxwell Fluid Flow in Rotating Frame," Journal of Nanofluids, **10**(1), 67–74 (2021). https://doi.org/10.1166/jon.2021.1767
[29] A. Anjum, S. Masood, M. Farooq, N. Rafiq, and M.Y. Malik, "Investigation of binary chemical reaction in magnetohydrodynamic nanofluid flow with double stratification," Adv. Mech. Eng. **13**(5), (2021). https://doi.org/10.1177/16878140211016264
[30] A.K. Gautam, A.K. Verma, K. Bhattacharyya, S. Mukhopadhyay, and A.J. Chamkha, "Impacts of activation energy and binary chemical reaction on MHD flow of Williamson nanofluid in Darcy–Forchheimer porous medium: a case of expanding sheet of variable thickness," Waves in Random and Complex Media, (2021). https://doi.org/10.1080/17455030.2021.1979274
[31] B. Saidulu, and K.S. Reddy, "Evaluation of Combined Heat and Mass Transfer in Hydromagnetic Micropolar Flow along a Stretching Sheet when Viscous Dissipation and Chemical Reaction Is Present," Partial Differential Equations in Applied Mathematics, **7**, 100467 (2023). https://doi.org/10.1016/j.padiff.2022.100467
[32] S.U. Rehman, A. Mariam, A. Ullah, M.I. Asjad, M.Y. Bajuri, B.A. Pansera, and A. Ahmadian, "Numerical Computation of Buoyancy and Radiation Effects on MHD Micropolar Nanofluid Flow over a Stretching/Shrinking Sheet with Heat Source," Case Studies in Thermal Engineering, **25**, 100867 (2021). https://doi.org/10.1016/j.csite.2021.100867
[33] D. Rees, and I. Pop, "Free convection boundary-layer flow of a micropolar fluid from a vertical flat plate," IMA Journal of Applied Mathematics, **61**(2), 179-197 (1998). https://doi.org/10.1093/imamat/61.2.179
[34] L.J. Grubka, and K.M. Bobba, "Heat Transfer Characteristics of a Continuous, Stretching Surface with Variable Temperature". ASME J. Heat Transfer, **107**, 248-250 (1985). http://dx.doi.org/10.1115/1.3247387
[35] M.A. Seddeek, and A.M. Salem, "Laminar mixed convection adjacent to vertical continuously stretching sheets with variable viscosity and variable thermal diffusivity," Heat Mass Transf. **41**, 1048–1055 (2005). http://dx.doi.org/10.1007/s00231-005-0629-6

ВПЛИВ ЕНЕРГІЇ АКТИВАЦІЇ АРРЕНІУСА В МГД ПОТОЦІ МІКРОПОЛЯРНОЇ НАНОРІДИНИ ВЗДОВЖ ПОРИСТОГО РОЗТЯГНУТОГО ЛИСТА З В'ЯЗКОЮ ДИСИПАЦІЄЮ І ДЖЕРЕЛОМ ТЕПЛА

Кешаб Борах[a], Джадав Конч[b], Шьяманта Чакраборти[c]

[a] *Департамент математики, Університет Гаухаті, Гувахаті-781014, Ассам, Індія*

[b] *Департамент математики, коледж Демаджі, Демаджі-787057, Ассам, Індія*

[c] *UGC-Центр розвитку персоналу, Університет Гаухаті, Гувахаті-781014, Ассам, Індія*

У цьому дослідженні проведено чисельне дослідження тепло- та масообміну потоку мікрополярного нанофлюїду над розтягнутим листом, вбудованим у пористе середовище. Основною метою цієї роботи є дослідження впливу енергії активації Арреніуса, джерела тепла та в'язкої дисипації на швидкість рідини, мікрообертання, температуру та розподіл концентрації. Рівняння, що керують потоком, перетворюються на звичайні диференціальні рівняння за допомогою відповідних перетворень подібності та розв'язуються чисельно за допомогою розв'язувача bvp4c у MATLAB. Графіки будуються для вивчення впливу важливих параметрів, таких як магнітний параметр, параметр пористості, параметр термофорезу, параметр броунівського руху, параметр енергії активації та число Льюїса на швидкість, мікрообертання, температуру та розподіл концентрації. Графічне представлення показує, що швидкість рідини зменшується зі збільшенням значень магнітного параметра, тоді як кутова швидкість збільшується разом із ним. Це дослідження також повідомляє, що посилення розподілу температури та концентрації спостерігається для більш високих значень параметра енергії активації, тоді як число Льюїса демонструє протилежну поведінку. Вплив різних відповідних параметрів реалістично відображено на коефіцієнті поверхневого тертя, числах Нуссельта та Шервуда за допомогою таблиць. Проведено порівняння з попередньою роботою, і результати показали хороший збіг.

Ключові слова: *енергія активації Арреніуса; в'язке розсіювання; броунівський рух; термофорез; мікрополярний нанофлюїд; пористе середовище*